COMBINED EFFECTS OF RADIATION AND JOULE HEATING WITH VISCOUS DISSIPATION ON MAGNETOHYDRODYNAMIC FREE CONVECTION FLOW AROUND A SPHERE

Miraj Akand[1], Md Abdul Alim[2*], Laek Sazzad Andallah[3], and Md Rezaul Karim[4]

Received: April 27, 2012; Revised: February 12, 2013; Accepted: February 15, 2013

Abstract

The effects of radiation and joule heating with viscous dissipation on magnetohydrodynamic (MHD) free convection flow around a sphere have been studied in this paper. The governing equations are transformed into dimensionless non-similar equations by using a set of suitable transformations and solved numerically by the finite difference method along with Newton's linearization approximation. The solutions are expressed in terms of the skin friction coefficient, the rate of heat transfer, the velocity profiles, and temperature profiles over the whole boundary layer. The effects of pertinent parameters such as radiation parameter Rd, viscous dissipation parameter Vd, magnetic parameter M, joule heating parameter J, and the Prandtl number Pr are shown graphically and discussed.

Keywords: Natural convection, radiation, prandtlnumber, joule heating parameter, viscous dissipation parameter, magnetohydrodynamics

Introduction

The phenomenon of the free convection boundary layer flow of an electrically conducting fluid on various geometrical shapes in the presence of a magnetic field is very common because of the applications in many engineering fields in connection with the cooling of reactors. It is usual to prescribe either the wall temperature or the wall heat flux and many researches have been done in order to understand the heat transfer characteristics over a wide range of flow configurations and fluid properties. But in many real engineering systems the wall conduction resistance cannot be neglected since conduction in the wall affects significantly the fluid flow and the heat

[1] *Department of Mathematics, Dhaka Commerce College, Dhaka-1216, Bangladesh.*
[2] *Department of Mathematics, Bangladesh University of Engineering and Technology, Dhaka- 10000, Bangladesh. E-mail: a0alim@gmail.com*
[3] *Department of Mathematics, Jahangirnagar University, Savar, Dhaka, Bangladesh.*
[4] *Department of Mathematics, Jagannath University, Dhaka, Bangladesh. E-mail: rrezaul@yahoo.com*
* *Corresponding author*

transfer characteristics of the fluid in the vicinity of the wall. The problems of free convection boundary layer flow along various types of geometrical shapes have been studied by many researchers. Amongst them Nazar *et al*. (2002) studied the free convection boundary layer on an isothermal sphere in a micropolar fluid. Huang and Chen (1987) considered the free convection boundary layer on an isothermal sphere and on an isothermal horizontal circular cylinder both in a micropolar fluid. Takhar and Soundalgekar (1980) studied the dissipation effects on magnetohydrodynamic (MHD) free convection flow past a semi-infinite vertical plate. Akhter and Alim (2008) studied the effects of radiation on natural convection flow around a sphere with a uniform surface heat flux. Limitations of this approximation are discussed briefly in Özisik (1973). The transformed boundary layer equations are solved numerically using the Keller box scheme describe by Keller (1978) and later by Cebeci and Bradshaw (1984) along with Newton's linearization approximation. Hossain (1992) analyzed the effect of viscous and joule heating on the flow of an electrically conducting fluid past a semiinfinite plate in which the temperature varies linearly with the distance from the leading edge and in the presence of a transverse magnetic field. In his paper, the finite difference method has been used to solve the equations governing the flow and the numerical solutions were obtained for small Prandtl numbers, appropriate for coolant liquid metal, in the presence of a large magnetic field. Miraj *et al.* (2010) and (2011) studied the effects of radiation and joule heating on MHD free convection flow along a sphere with heat generation. Molla *et al.* (2005) studied the problem of MHD natural convection flow on a sphere in the presence of heat generation or absorption. Alam *et al.* (2007) studied the viscous dissipation effects with MHD natural convection flow on a sphere in the presence of heat generation. El-Amin (2003) also analyzed the influences of both first and second order resistance, due to the solid matrix of a non-Darcy porous medium, joule heating, and viscous dissipation on a forced convection flow from a horizontal circular cylinder under the action of a transverse magnetic field. The present study is to incorporate the idea of the effects of radiation and joule heating on MHD free convection flow around a sphere with viscous dissipation. The numerical results in terms of local skin friction, rate of heat transfer, velocity profiles, as well as temperature profiles for different values of relevant physical parameters are presented graphically.

Formulation of the Problem

A steady 2-dimensional MHD natural convection boundary layer flow from an isothermal sphere of radius a, which is immersed in a viscous and incompressible optically dense fluid with radiation heat loss is considered. Let us consider that the surface temperature of the sphere with radius a where Tw is the constant temperature (Tw > T∞), T is the ambient temperature of the fluid, T is the temperature of the fluid in the boundary layer, g is the acceleration due to gravity, and (U, V) are velocity components along the (X, Y) axes. The physical configuration considered is as shown in Figure 1.

According to the above assumption, the governing Equations' continuity, momentum, and energy for a steady 2-dimensional laminar boundary layer flow problem under consideration can be written as:

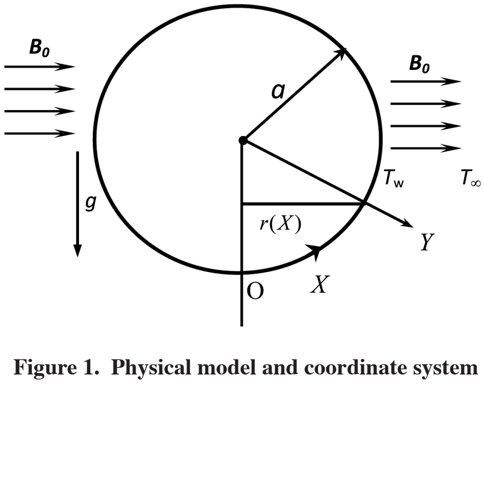

Figure 1. Physical model and coordinate system

$$\frac{\partial}{\partial X}(rU)+\frac{\partial}{\partial Y}(rV)=0 \tag{1}$$

$$U\frac{\partial U}{\partial X}+V\frac{\partial U}{\partial Y}=\nu\frac{\partial^2 U}{\partial Y^2}+g\beta(T-T_\infty)\sin\left(\frac{X}{a}\right)-\frac{\sigma_0 B_0^{\,2}}{\rho}U \tag{2}$$

$$U\frac{\partial T}{\partial X}+V\frac{\partial T}{\partial Y}=\frac{k}{\rho c_p}\left(\frac{\partial^2 T}{\partial Y^2}-\frac{1}{k}\frac{\partial q_r}{\partial Y}\right)+\frac{\nu}{\rho c_p}\left(\frac{\partial U}{\partial Y}\right)^2+\frac{\sigma_0 B_0^{\,2}}{\rho c_p}U^2 \tag{3}$$

with the boundary conditions:

$$\begin{aligned} &U=V=0,\ T=T_w\ \ at\ Y=0 \\ &U\to 0,\ T\to T_\infty\ \ as\ Y\to\infty \end{aligned} \tag{4}$$

where $r(X)=a\sin\left(X/a\right)$ is the radial distance from the symmetrical axis to the surface of the sphere, k is the thermal conductivity, β is the coefficient of thermal expansion, B_0 is the strength of magnetic field, σ_0 is the electricalconductivity, ν (= μ/ρ) is the kinematic viscosity, μ is the viscosity of the fluid, ρ is the density, and cpis the specific heat due to constant pressure.

The above equations are non-dimensionalised using the following new variables:

$$\xi=\frac{X}{a},\quad \eta=\frac{Y}{a}Gr^{\frac{1}{4}},\ u=\frac{aU}{\nu}Gr^{-\frac{1}{2}},\ v=\frac{aV}{\nu}Gr^{-\frac{1}{4}} \tag{5}$$

$$\theta=\frac{T-T_\infty}{T_w-T_\infty},\ \ Gr=g\beta(T_w-T_\infty)\frac{a^3}{\nu^2} \tag{6}$$

$$\theta_w=\frac{T_w}{T_\infty},\ \Delta=\theta_w-1=\frac{T_w}{T_\infty}-1=\frac{T_w-T_\infty}{T_\infty} \tag{7}$$

where Gr is the Grashof number, θ is the non-dimensional temperature function, and θ_w is the surface temperature parameter.

The Rosseland diffusion approximation proposed by Siegel and Howell (1972) is given by the simplified radiation heat flux term as:

$$q_r=-\frac{4\sigma}{3(a_r+\sigma_s)}\frac{\partial T^4}{\partial Y} \tag{8}$$

where a_r is the Rosseland mean absorption co-efficient, σ_s is the scattering co-efficient, and σ is the Stefan-Boltzmann constant.

Substituting (5), (6), and (7) in the continuity Equation (1), the momentum Equation (2), and the energy Equitation (3) leads to the following non-dimensional Equations:

$$\frac{\partial}{\partial\xi}(ru)+\frac{\partial}{\partial\eta}(rv)=0 \tag{9}$$

$$u\frac{\partial u}{\partial\xi}+v\frac{\partial u}{\partial\eta}=\frac{\partial^2 u}{\partial\eta^2}+\theta\sin\xi-\frac{\sigma_0 B_0^{\,2}a^2}{\rho\nu Gr^{\frac{1}{2}}}u \tag{10}$$

$$u\frac{\partial\theta}{\partial\xi}+v\frac{\partial\theta}{\partial\eta}=\frac{1}{Pr}\frac{\partial}{\partial\eta}\left[\left\{1+\frac{4}{3}Rd\left(1+(\theta_w-1)\theta\right)^3\right\}\frac{\partial\theta}{\partial\eta}\right] +Vd\left(\frac{\partial u}{\partial\eta}\right)^2+Ju^2 \tag{11}$$

where $Pr=\dfrac{\mu c_p}{k}$ is the Prandtl number, $J=\dfrac{\sigma_0 B_0^2\nu}{\rho c_p(T_w-T_\infty)}$ is the joule heating parameter, $Vd=\dfrac{\nu^2 Gr}{\rho a^2 c_p(T_w-T_\infty)}$ is the viscous dissipation, and $Rd=\dfrac{4\sigma\ T_\infty^3}{k(a_r+\sigma_s)}$ is the radiation parameter.

With the boundary conditions (4) become

$$\begin{aligned} &u=v=0,\ \theta=1\ \text{ at }\ \eta=0 \\ &u\to 0,\ \theta\to 0\ \text{ as }\ \eta\to\infty \end{aligned} \tag{12}$$

to solve Equations (10) and (11) with the help of following variables:

$$\psi=\xi\ \ r(\xi)f(\xi,\eta)\ ,\ \theta=\theta(\xi,\eta),\ r(\xi)=\sin\xi \tag{13}$$

where ψ is the stream function defined by:

$$u=\frac{1}{r}\frac{\partial\psi}{\partial\eta},\ v=-\frac{1}{r}\frac{\partial\psi}{\partial\xi} \tag{14}$$

Using the above values in Equitation (10), we get the following Equation:

$$\frac{\partial^3 f}{\partial\eta^3}+\left(1+\frac{\xi}{\sin\xi}\cos\xi\right)f\frac{\partial^2 f}{\partial\eta^2}+\theta\frac{\sin\xi}{\xi}-\left(\frac{\partial f}{\partial\eta}\right)^2- M\frac{\partial f}{\partial\eta}=\xi\left(\frac{\partial f}{\partial\eta}\frac{\partial^2 f}{\partial\xi\partial\eta}-\frac{\partial f}{\partial\xi}\frac{\partial^2 f}{\partial\eta^2}\right) \tag{15}$$

where $M-\dfrac{\sigma_0 B_0^{\,2}a^2}{\mu Gr^{1/2}}$ is the MHD parameter

Putting the values of u and v in Equation

(11), we get the following Equation:

$$\frac{1}{Pr}\frac{\partial}{\partial\eta}\left\{\left(1+\frac{4}{3}Rd(1+(\theta_w-1)\theta)^3\right)\frac{\partial\theta}{\partial\eta}\right\}+\left(1+\frac{\xi}{\sin\xi}\cos\xi\right)f\frac{\partial\theta}{\partial\eta}$$
$$+Vd\xi^2\left(\frac{\partial^2 f}{\partial\eta^2}\right)^2+J\xi^2\left(\frac{\partial f}{\partial\eta}\right)^2=\xi\left(\frac{\partial f}{\partial\eta}\frac{\partial\theta}{\partial\xi}-\frac{\partial\theta}{\partial\eta}\frac{\partial f}{\partial\xi}\right) \quad (16)$$

along with boundary conditions

$$f=f'=0,\ \theta=1 \ \text{ at } \ \eta=0$$
$$f'\to 0,\ \theta\to 0 \ \text{ as } \ \eta\to\infty \quad (17)$$

where primes denote the differentiation of the function with respect to η.

It can be seen that near the lower stagnation point of the sphere, i.e., $\xi \approx 0$, Equations (15) and (16) reduce to the following ordinary differential Equations:

$$f'''+2ff'-f'^2+\theta-Mf'=0 \quad (18)$$

$$\frac{1}{Pr}\left[\left\{1+\frac{4}{3}Rd\left(1+(\theta_w-1)\theta\right)^3\right\}\theta'\right]'+2f\theta'=0 \quad (19)$$

subject to the boundary conditions;

$$f(0)=f'(0)=0,\ \theta(0)=1$$
$$f'\to 0,\ \theta\to 0 \ \text{ as } \ \eta\to\infty \quad (20)$$

In practical applications, the physical quantities of principle interest are the shearing stress τ_w, the rate of heat transfer, and the rate of species concentration transfer in terms of the skin friction coefficient C_f and Nusselt number Nu, which can be written in non-dimensional form as:

$$C_f=\frac{a^2Gr^{-\frac{3}{4}}}{\mu\nu}\tau_w \ \text{ and } \ Nu \ \frac{aGr^{-\frac{1}{4}}}{k(T_w-T_\infty)}\left(q_c+q_r\right)_{Y=0} \quad (21)$$

where $\tau_w=\mu\left(\frac{\partial U}{\partial Y}\right)_{Y=0}$ is the shearing stress, $q_c=-k\left(\frac{\partial T}{\partial Y}\right)_{Y=0}$ is the conduction heat flux, k being the thermal conductivity of the fluid, and q_r is the radiation heat flux. The heat flux q_r is defined by:

$$q_w=(q_c)_{Y=0}+(q_r)_{Y=0}=-k\left(\frac{\partial T}{\partial Y}\right)_{Y=0}+q_{r\ \ Y=0}$$

Using Equations (5) and (6), boundary condition (20) and putting the values of τ_w and q_r in (21), we get the following Equations:

$$Nu=-\left(1+\frac{4}{3}Rd\theta_w^{\ 3}\right)\theta'(\xi,0) \quad (22)$$

$$C_f=\xi f''(\xi,0) \quad (23)$$

The values of the velocity and temperature distribution are calculated respectively from the following relations:

$$u=\frac{\partial f}{\partial\eta}, \quad \theta=\theta(\xi,\eta)$$

We discuss the velocity distribution as well as the temperature profiles for a selection of relevant parameters.

Method of Solution

The finite-difference methods are numerical methods for approximating the solutions to differential equations using finite difference equations to approximate derivatives. The governing partial differential equations are reduced to dimensionless local non-similar equations by adopting appropriate transformations. The transformed boundary layer equations are solved numerically using in-house FORTRAN code based on the Keller box method. The partial differential Equations (15) and (16) are first converted into a system of first order differential equations. These equations are expressed in finite difference forms by approximating the functions and their derivatives in terms of the centered differences and 2 point averages using only values at the corner of the box (or mesh rectangle). Denoting the mesh points in the (ξ, η)-plane by ξ_i and η_j where $i = 1, 2, \ldots,$ M and j = 1, 2, . . . , N, central difference approximations are made, such that those equations involving ξ explicitly are centered at ($\xi_{i-1/2}$, $\eta_{j-1/2}$) and the remainder at (ξ_i , $\eta_{j-1/2}$), where $\eta_{j-1/2} = \frac{1}{2}(\eta_j + \eta_{j-1})$ etc. Grid dependency has been tested and solutions are obtained with a grid of optimum dimensions 182×200 in the (ξ, η) domain and a non-uniform mesh size is employed to produce results of high accuracy near the coordinate $\xi = 0$, $\eta = 0$. The central difference approximations reduce the system of first order differential equations to a set of non-linear difference equations for the unknown at ξ_i in terms of their values at ξ_{i-1}. The resulting set of nonlinear difference equations are solved by using the Newton's quasi-linearization method. The Jacobian matrix has a block-tridiagonal structure and the difference equations are solved using a block-matrix version of the Thomas algorithm; further details of the computational procedure have been discussed in the book by Cebeci and Bradshaw (1984) and widely used by many authors including Hossain (1992).

Results and Discussion

Solutions are obtained in terms of velocity profiles, temperature profiles, skin friction coefficient, and rate of heat transfer and presented graphically for selected values of the radiation parameter *Rd*, Prandtl number *Pr*, magnetic parameter *M*, joule heating parameter *J*, and viscous dissipation parameter *Vd*. The effects for different values of the radiation parameter (*Rd* = 1.00, 3.00, 5.00, 7.00, 9.00), the velocity profiles, and temperature profiles in the case of the Prandtl number *Pr* = 0.72, magnetic parameter *M* = 0.50, joule heating parameter *J* = 0.30, and viscous dissipation parameter *Vd* = 25.00 are shown in Figures 2(a) and 2(b), respectively. We observe that, when the radiation parameter *Rd* increases, both the velocity and the temperature profiles increase such that there exists a local maximum of the velocity within the boundary layer but the velocity increases near the surface of the sphere and then the temperature increases slowly and finally approaches to 0. In Figure 2(a) we observed that the velocity boundary layer thickness increases. The thermal boundary layer thickness increases for the increasing values of the radiation parameter *Rd*. The increasing values of the Prandtl number (*Pr* = 0.72, 1.50, 3.00, 4.00, 7.00), the velocity profiles, and the temperature profiles decrease are shown in Figures 3(a) and 3(b), respectively. The velocity boundary layer thickness and thermal boundary layer thickness decrease for the increasing values of Prandtl number *Pr*.

In Figure 4(a), it is shown that the magnetic field action along the horizontal direction retards the fluid velocity with the radiation parameter *Rd* = 1.00, Prandtl

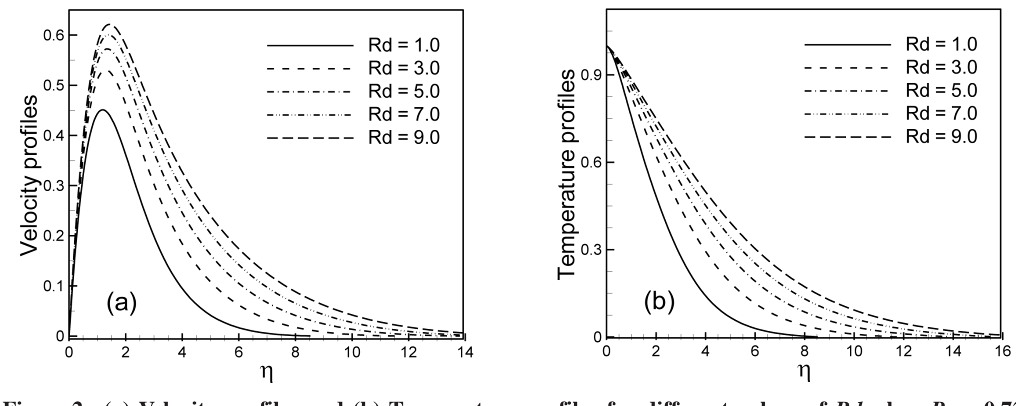

Figure 2. (a) Velocity profiles and (b) Temperature profiles for different values of *Rd* when *Pr* = 0.72, *M* = 0.5, *J* = 0.3, and *Vd* = 25.0

number Pr = 0.72, joule heating parameter J = 0.30, and viscous dissipation parameter Vd = 25.00. Here, the position of peak velocity moves toward the interface with increasing the values of M, so the velocity boundary layer decreases for increasing the values of M. From Figure 4(b), it can be observed that the temperature within the boundary layer increases for increasing the values of M from 0.10 to 1.80.

Figures 5(a) and 5(b) display that, for the results of the velocity and temperature profiles, for different values of the joule heating parameter (J = 0.30, 4.00, 8.00, 12.00, 15.00) with radiation parameter Rd = 1.00, Prandtl number Pr = 0.72, magnetic parameter M = 2.00, and viscous dissipation parameter Vd =25.00, the joule heating parameter J increases, the velocities rise up to the position of η = 1.23788, and from that the position of η velocities falls down slowly and finally approaches to 0. It is also observed from Figure 5(b) that as the joule heating parameter J increases, the temperature profiles increase. Figures 6(a) and 6(b) display the results that, for the increasing values of the viscous dissipation parameter (Vd = 0.10, 25.00, 50.00, 75.00, 100.00), both the velocity profiles and temperature profiles increase.

It has been seen from Figure 7(a) that as the radiation parameter Rd increases, the skin friction coefficient C_f increases up to the

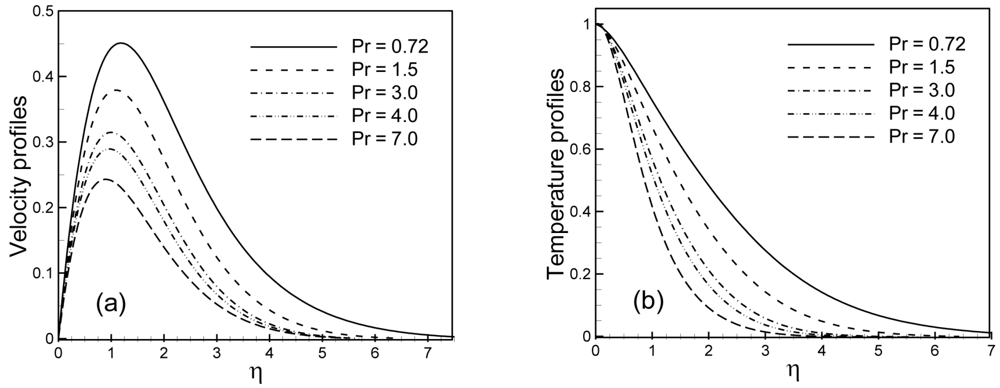

Figure 3. (a) Velocity profiles and (b) Temperature profiles for different values of *Pr* when *Rd* = 1.0, *M* = 0.5, *J* = 0.3, and *Vd* = 25.0

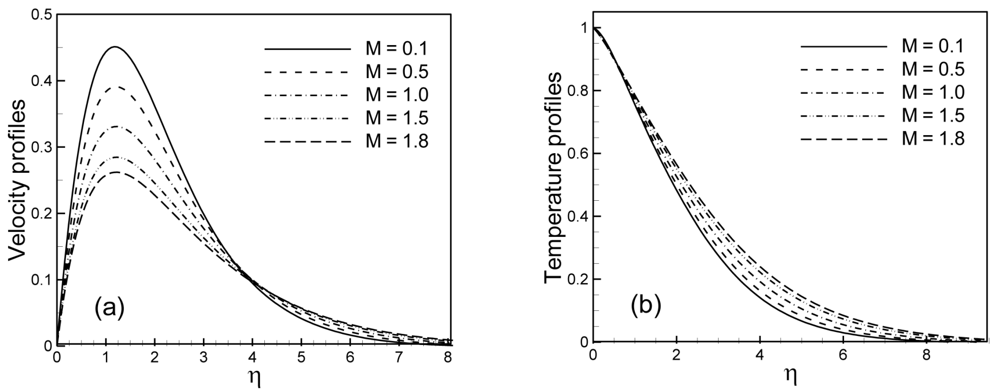

Figure 4. (a) Velocity profiles and (b) Temperature profiles for different values of *M* when *Rd* = 1.0, *Pr* = 0.72, *J* = 0.3, and *Vd* = 25.0

position of $\xi = 1.08210$ and from that position the skin friction coefficient C_f decreases and the rate of heat transfer Nu increases, as shown in the Figure 7(b). In Figure 8(a) it is shown that when the Prandtl number Pr increases, the skin friction coefficient C_f decreases up to the position of $\xi = 0.89012$ and from that position of ξ the skin friction coefficient C_f changes with the increasing values of the Prandtl number Pr. It has been seen from Figure 8(b) that as the Prandtl number Pr increases, the rate of heat transfer Nu increases up to the position of $\xi = 0.31416$ and from that position of ξ the rate of heat transfer decreases. Due to the combined effects of viscous dissipation with heat generation and higher radiation, the rate of heat transfer Nu is higher initially but the temperature falls down quickly for higher radiation and temperature differences between the wall and fluid as well as the rate of heat transfer Nu reduces. For a lower radiation, the rate of heat transfer Nu is lower initially but the temperature falls down slowly and the rate of heat transfer Nu decreases slowly. Eventually, the rate of heat transfer lines meet at a certain point and cross the sides. In Figure 9(a), with the increasing values of magnetic parameter M, the skin friction coefficient C_f decreases. It is observed from Figure 9(b), that the rate of heat transfer decreases up to the same position of ξ and then the rate of heat transfer increases

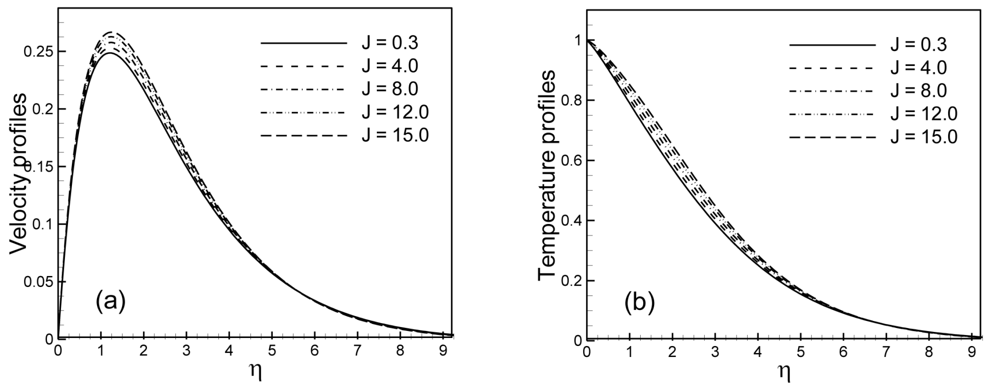

Figure 5. (a) Velocity profiles and (b) Temperature profiles for different values of J when Rd = 1.0, Pr = 0.72, M = 2.0, and Vd = 25.0

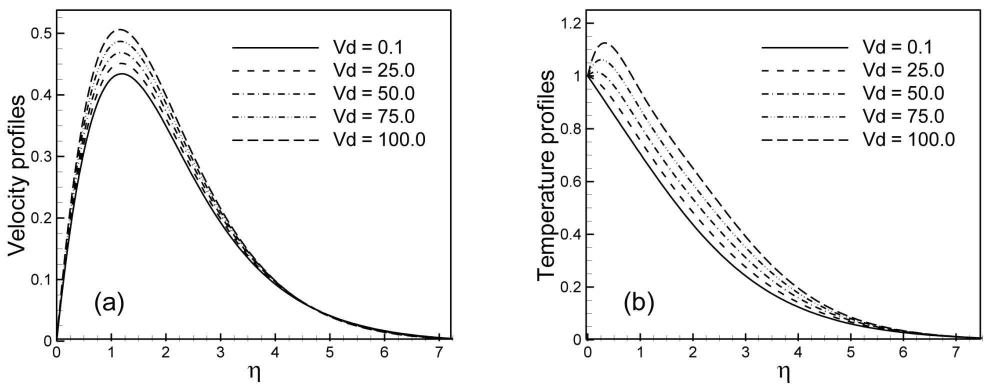

Figure 6. (a) Velocity profiles and (b) Temperature profiles for different values of Vd when Rd = 1.0, Pr = 0.72, M = 0.5, and J = 0.3

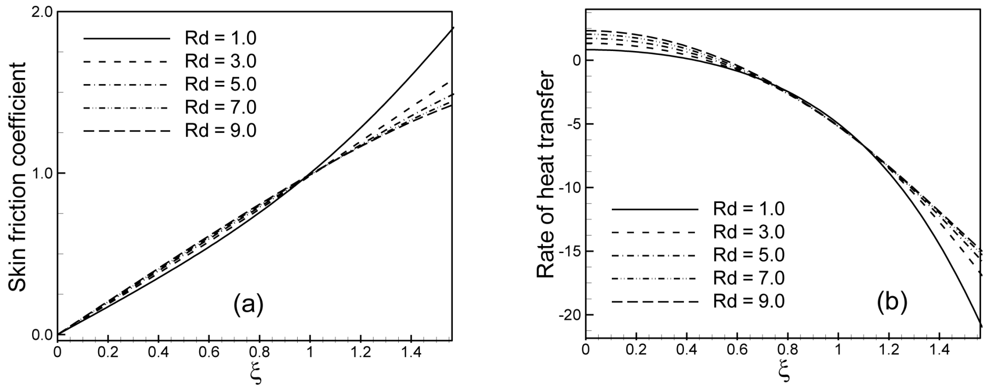

Figure 7. **(a) Skin friction coefficient and (b) Rate of heat transfer for different values of C_f when $Pr = 0.72$, $M = 0.5$, $J = 0.3$, and $Vd = 25.0$**

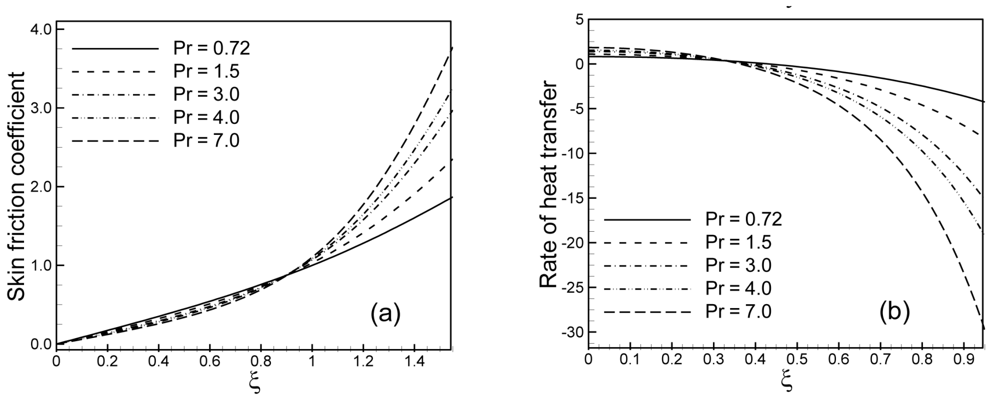

Figure 8. **(a) Skin friction coefficient and (b) Rate of heat transfer for different values of Pr when $Rd = 1.0$, $M = 0.5$, $J = 0.3$, and $Vd = 25.0$**

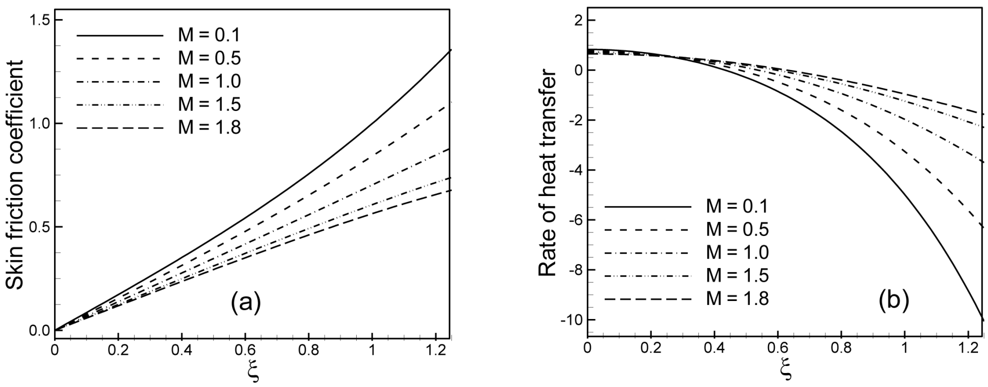

Figure 9. **(a) Skin friction coefficient and (b) Rate of heat transfer for different values of Q when $Rd = 1.0$, $Pr = 0.72$, $J = 0.3$, and $Vd = 25.0$**

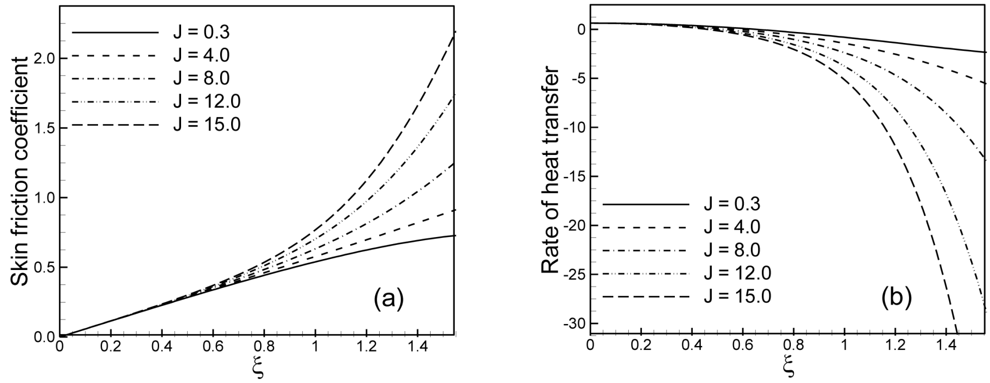

Figure 10. (a) Skin friction coefficient and (b) Rate of heat transfer for different values of *J* when *Rd* = 1.0, *Pr* = 0.72, *M* = 2.0, and *Vd* = 25.0

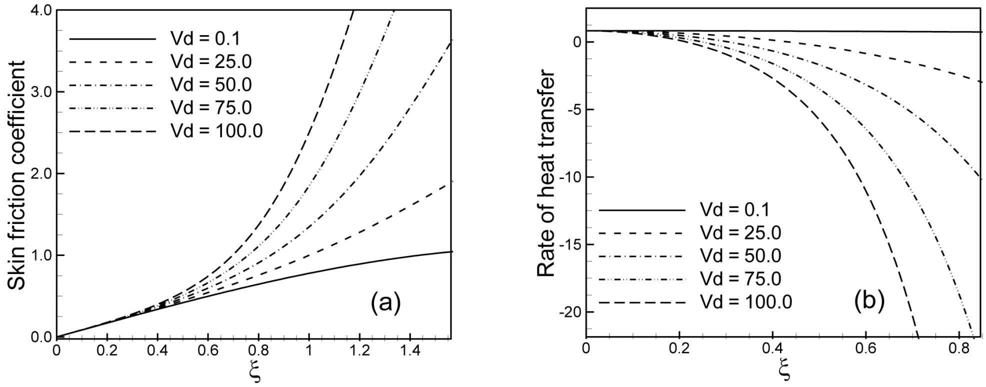

Figure 11. (a) Skin friction coefficient and (b) Rate of heat transfer for different values of *Vd* when *Rd* = 1.0, *Pr* = 0.72, *M* = 0.5, and *J* = 0.3

for increasing values of the magnetic parameter *M*. From Figures 10(a) and 10(b) we observed that the skin friction coefficient Cfincreases and the heat transfer coefficient decreases for increasing values of the joule heating parameter *J* with radiation parameter *Rd* = 1.00, Prandtl number *Pr* = 0.72, magnetic parameter *M* = 2.00, and viscous dissipation parameter *Vd* =25.00. Figure 11(a) shows the skin friction coefficient C_f increases for increasing values of the viscous dissipation parameter *Vd* with radiation parameter *Rd* = 1.00, Prandtl number *Pr* = 0.72, magnetic parameter *M* = 0.50, and joule heating parameter *J* = 0.30. Frictional force at the wall becomes much higher towards the downstream for higher values of *Vd* and the rate of heat transfer, as shown in Figure 11(b), gradually decreased for higher values of the viscous dissipation parameter.

Comparison of the Results

The comparison of the present numerical results of the rate of heat transfer *Nu* with those obtained by Nazar *et al*. (2002) and Huang and Chen (1987) is shown in Table 1. Here, the magnetic parameter *M*, radiation parameter *Rd*, joule heating parameter *J*, and viscous dissipation parameter *Vd* are ignored

Table 1. Comparison of numerical results with those obtained by Huang and Chen (1987) and Nazar *et al.* (2002)

ξ in degree	*Pr* = 0.70			*Pr* = 7.00		
	Nazar *et al.* (2002)	Huang and Chen (1987)	Present results	Nazar *et al.* (2002)	Huang and Chen (1987)	Present results
0	0.4576	0.4574	0.4577	0.9595	0.9581	0.9564
10	0.4565	0.4563	0.4566	0.9572	0.9559	0.9542
20	0.4533	0.4532	0.4533	0.9506	0.9496	0.9477
30	0.4480	0.4480	0.4480	0.9397	0.9389	0.9389
40	0.4405	0.4407	0.4406	0.9239	0.9239	0.9218
50	0.4308	0.4312	0.4310	0.9045	0.9045	0.9022
60	0.4189	0.4194	0.4191	0.8801	0.8805	0.8781
70	0.4046	0.4053	0.4049	0.8510	0.8518	0.8493
80	0.3879	0.3886	0.3883	0.8168	0.8182	0.8154
90	0.3684	0.3694	0.3690	0.7774	0.7792	0.7763

and the Prandtl numbers $Pr = 0.70$ and 7.00 are chosen. The present results agreed well with the solutions of Nazar *et al.* (2002) in the absence of the micropolar parameter and of Huang and Chen (1987) in the absence of suction and blowing. This comparison is shown in the following Table1.

Conclusions

The present investigation focuses on the effects of radiation and joule heating with viscous dissipation on MHD free convection flow around a sphere. Velocity profiles increase for increasing values of the radiation parameter Rd, joule heating parameter J, and viscous dissipation parameter Vd. Temperature profiles increase for increasing values of radiation parameter Rd, magnetic parameter M, joule heating parameter J, and viscous dissipation parameter Vd. Velocity profiles and temperature profiles decrease for increasing values of the Prandlt number Pr. Skin friction coefficients C_f increase for increasing values of the joule heating parameter J and viscous dissipation parameter Vd. Skin friction coefficients C_f decrease for increasing values of the magnetic parameter M. The rate of heat transfer Nu increases for increasing values of the radiation parameter Rd and the rate of heat transfer Nu decreases for increasing values of the joule heating parameter J and viscous dissipation parameter Vd.

Nomenclature

a	–	Radius of the sphere [m]
a_r	–	Rosseland mean absorption co-efficient [cm^3/s]
B_0	–	Strength of magnetic field [A/m]
C_f	–	Skin-friction coefficient
C_P	–	Specific heat at constant pressure [Jkg^{-1}k^{-1}]
f	–	Dimensionless stream function
g	–	Acceleration due to gravity [ms^{-2}]
Gr	–	Grashof number
J	–	Joule heatingparameter [–]
k	–	Thermal conductivity [wm^{-1}k^{-1}]
M	–	Magnetic parameter [–]
Nu	–	Nusselt number [–]
Pr	–	Prandtl number [–]
q_c	–	Conduction heat flux [w/m^2]
q_r	–	Radiative heat flux [w/m^2]
q_w	–	Heat flux at the surface [w/m^2]
Rd	–	Radiation parameter [–]
r	–	Radial distance from the symmetric axis to the surface [m]

T – Temperature of the fluid in the boundary layer [K]
T_∞ – Temperature of the ambient fluid [K]
T_w – Temperature at the surface [K]
U – Velocity component along the surface [ms^{-1}]
V – Velocity component normal to the surface [ms^{-1}]
u – Dimensionless velocity along the surface [–]
v – Dimensionless velocity normal to the surface [–]
Vd – Viscous dissipation parameter [–]
X – Coordinate along the surface [m]
Y – Coordinate normal to the surface [m]

Greek Symbols

β – Coefficient of thermal expansion [K^{-1}]
θ – Dimensionless temperature [–]
μ – Dynamic viscosity of the fluid [kgm-1s^{-1}]
ν – Kinematic viscosity [m^2/s]
ρ – Density of the fluid [kgm^{-3}]
σ – Stefan Boltzmann constant [$js^{-1}\, m^{-2}\, k^{-4}$]
σ_0 – Electrical conductivity [mho.m^{-1}]
σ_s – Scattering coefficient [m^{-1}]
τ_w – Shearing stress at the wall [N/m^2]
ξ – Dimensionless coordinate along the surface [–]
η – Dimensionless coordinate normal to the surface [–]
Ψ – Stream function [m^2s^{-1}]

References

Akhter, T. and Alim, M.A. (2008). Effects of radiation on natural convection flow around a sphere with uniform surface heat flux. J. Mech. Eng., 39(1):50-56. Available from: http://www.banglajol.info/index.php/JME/article/view/1834.

Alam, M.M., Alim, M.A., and Chowdhury, M.M.K. (2007). Viscous dissipation effects with MHD natural convection flow on a sphere in the presence of heat generation. Nonlinear Analysis: Modelling and Control, 12(4):447-459.

Cebeci, T. and Bradshaw, P. (1984). Physical and Computational Aspects of Convective Heat Transfer. 1st ed. Springer-Verlag, NY, USA, 487p.

El-Amin, M.F. (2003). Combined effect of viscous dissipation and Joule heating on MHD forced convection over a non-isothermal horizontal cylinder embedded in a fluid saturated porous medium, J. Magn. Magn. Mater., 263:337-343.

Hossain, M.A. (1992). The viscous and Joule heating effects on MHD free convection flow with variable plate temperature. Int. J. Heat Mass Tran., 35(12):3485-3487.

Huang, M.J. and Chen, C.K. (1987). Laminar free convection from a sphere with blowing and suction. J. Heat Transf., 109:529-532.

Keller, H.B. (1978). Numerical methods in boundary layer theory. Annu. Rev. Fluid Mech., 10:417-433.

Miraj, M., Alim, M.A., and Mamun, M.A.H. (2010). Effect of radiation on natural convection flow on a sphere in the presence of heat generation. Int. Commun. Heat Mass, 37(6):660-665.

Miraj Ali, M., Alim, M.A. and Andallah, L.S. (2011). Conjugate effects of radiation and joule heating on magnetohydrodynamicfree convection flow along a sphere with heat generation. American J. Comp. Math., 1(1):18-25. Available from: http://www.scirp.org/journal/PaperDownload.aspx?paperID=4449

Molla, M.M., Taher, M.A., Chowdhury, M.M.K., and Hossain, M.A. (2005). Magnetohydrodynamic natural convection flow on a sphere in the presence of heat generation. Nonlinear Analysis: Modelling and Control, 10(4):349–363.

Nazar, R., Amin, N., Grosan., T., and Pop, I. (2002). Free convection boundary layer on an isothermal sphere in micropolar fluid. Int. Commun. Heat Mass, 29(3):377-386

Özisik, M.N. (1973). Radiative Transfer and Interactions with Conduction and Convection. 1st ed. Wiley, NY, USA, 575 p.

Siegel, R. and Howell, J.R. (1972). Thermal Radiation Heat Transfer. 1st ed. McGraw-Hill, NY, USA, 814p.

Takhar, H.S. and Soundalgekar, V.M. (1980). Dissipation effects on MHD free convection flow past a semi-infinite vertical plate. Appl. Sci. Res., 36(3):163-171.